

Supporting Information

The Study of Multireactional Electrochemical Interfaces Via a Tip Generation/Substrate

Collection Mode of Scanning Electrochemical Microscopy

The Hydrogen Evolution Reaction for Mn in Acidic Solution

Kevin C. Leonard^γ and Allen J. Bard^{*}

Center for Electrochemistry, Department of Chemistry and Biochemistry, University of Texas at

Austin, Austin, TX 78712

COMSOL Simulation Details

As stated in the main text, COMSOL simulations were performed to obtain the precise tip/substrate distance for the approach curves and the kinetics for proton reduction on Mn. Figure S1 shows the 3D geometry created to simulate the actual experimental setup. The entire domain was a cylinder with a radius and height of 5 mm. At the bottom of the cell geometry an additional work plane was created consisting of a 1 mm radius circle for the substrate electrode. The tip electrode was a rectangular cuboid with a width of 315 μm and a length of 345 μm surrounded by a 300 μm radius cylinder. In addition, to best simulate the real electrode, the rectangular cuboid (electrode) protruded out from the surrounding cylinder (insulation sheath) by 10 μm (Figure S1B). The mesh on the tip had a maximum element size of 2 μm with a minimum element size of 0.2 μm , while the mesh on the substrate had a maximum element size of 20 μm and a minimum element size of 2 μm . COMSOL's default extra fine mesh was used for the remainder of the geometry.

The concentration of H^+ and H_2 were determined throughout the geometry by solving Fick's Second Law of Diffusion (EQ S1) for both species.

^γ Current Address: Center for Environmentally Beneficial Catalysis; Department of Chemical & Petroleum Engineering; The University of Kansas; 4132B Learned Hall; 1530 W 15th St; Lawrence KS 66045

$$\frac{\partial C_O}{\partial t} = D_O \nabla^2 C_O \quad (\text{S1})$$

where D_O is the diffusion coefficient of the oxidized form and C_O is the concentration of the oxidized form. The diffusion coefficient and concentration of the reduced form D_R and C_R were used to determine the H_2 concentration profile. As stated in the main text, the diffusion coefficients used were $7.8 \times 10^{-5} \text{ cm}^2\text{s}^{-1}$ and $4.5 \times 10^{-5} \text{ cm}^2\text{s}^{-1}$ for H^+ and H_2 respectively. Reported values for the diffusion coefficient of H_2 in water vary from $4.5 \times 10^{-5} \text{ cm}^2\text{s}^{-1}$ to $5 \times 10^{-5} \text{ cm}^2\text{s}^{-1}$.^{1,2} Even though these values only differ by 10%, we found a slightly better fit to the experimental data using the value of $4.5 \times 10^{-5} \text{ cm}^2\text{s}^{-1}$. Using COMSOL's parametric sweep function the concentrations of H^+ and H_2 were determined for 13 different tip/substrate distances. For the approach curves, mass transfer controlled concentration boundary conditions were used on the tip and substrate electrodes.

The current on the tip and substrate electrode were calculated using Fick's First Law of Diffusion (EQ S2).

$$\frac{i}{nFA} = -J(t)|_{z=0} = D_O \frac{\partial C_O}{\partial z} |_{z=0} \quad (\text{S2})$$

where i is the current, n is the electron number, F is Faraday's constant, A is the electrode area, and J is the flux. For proton reduction on the tip electrode, the electron number was set to one because there is one electron transfer per H^+ . For H_2 oxidation on the substrate electrode, the electron number was set to two because there are two electron transfers per H_2 molecule.

Because of the size of our tip electrode, and the difference in diffusion coefficients, steady state may not be achieved during the approach curve when the SECM is in feedback mode. Martin & Unwin³ show that for a ratio of diffusion coefficients, γ , with

$$\gamma = \frac{D_O}{D_R} \quad (\text{S3})$$

steady state can be achieved for an SECM system under feedback when τ is between 2 and 3 for $d/a = 0.2$ with

$$\tau = \frac{t D_R}{a^2} \quad (\text{S4})$$

where t is time, d is the tip/substrate distance, and a is the radius of a disk electrode. Assuming our electrode has the same area as a disk electrode with $a = 185 \mu\text{m}$, Equations S3 and S4 would predict the time to steady state for our electrode is between 15 – 23 seconds. In our experiment, we achieve a tip/substrate distance of $65 \mu\text{m}$ which is an equivalent d/a of ~ 0.35 . For this d/a value we verified that steady state is reached before 15 seconds by calculating the tip current as a function of time for our 3D geometry under feedback at tip distance of $65 \mu\text{m}$ (Figure S2).

Because steady-state is reached by 15 seconds both as predicted by theory and by our simulations, the transient solver with a time step of 15 s was used for each tip/substrate distance. In general, as long as the time step is sufficiently long, the transient solver time does not have a dramatic effect on the tip current. However, since this system has a large tip electrode, and long distances for SECM (our approach curve covers $700 \mu\text{m}$), the transient solver time does have an impact on the substrate current because of the diffusion time between the tip and the substrate. In addition, 15 seconds was chosen for the transient solver time because it provided the best fit of our simulated substrate current to the experimental results.

To simulate the linear sweep voltammetry experiments, the tip/substrate distance was set to 65 μm as determined by the experimental approach curve. All geometry and mesh conditions were the same as the approach curve, however a flux boundary condition was now set on the tip electrode as shown in Equation S3.

$$J = -k_F \cdot C_O + k_b \cdot C_R \quad (\text{S3})$$

where k_F is the forward rate constant and k_b is the backward rate constant with

$$k_F = k^{\text{eff}} e^{-\alpha f \eta} \quad (\text{S4})$$

$$k_b = k^{\text{eff}} e^{(1-\alpha) f \eta} \quad (\text{S5})$$

where $f = F/RT$ and η is the overpotential. Since the scan rate of the tip electrode is sufficiently slow (1 mV s^{-1}) we used the steady-state solver to obtain simulation for the potential sweep experiments.

Because of the unique shape of our tip electrode, we utilized 3D geometries in our simulations to best represent our experimental systems. However, there are still a few spots of uncertainty which may slightly affect our final measurement. Our Mn tip electrode was hand polished and sharpened, and may have a small amount of surface roughness associated with it. Future studies on using nonconventional materials as the tip electrode may want to utilize focused ion beam (FIB) microstructuring techniques to produce more reliable electrode shapes.⁴ In addition, as with all SECM experiments, the tip may not be perfectly perpendicular to the substrate, as is the case with the simulation. This may also be a source of error in the kinetic determination, but is considered negligible for our purposes.

Proton Reduction on Fe using Multireactional TG/SC SECM

To verify the results we obtained for proton reduction on Mn, we also used the tip generation substrate collection mode of SECM to investigate proton reduction on Fe, another corrosive metal. Fe oxidation occurs at -0.44 V vs. NHE, but because of the sluggish kinetics, proton reduction on Fe is easier to measure than on Mn by conventional methods. However, it makes a good test case for our multireactional TG/SC SECM technique.

Similar to the Mn tip electrode, a custom Fe tip electrode was created for the multireactional SECM experiment. To create the tip, a 1.0 mm diameter Fe wire was electrochemically etched in 1 M HClO₄ with AC using a Variac autotransformer similar to a previously reported method.⁵ Current was applied to the Fe wire for approximately 5 min, the Fe wire was raised approximately 3 cm, and this process was repeated three times until the wire was sharpened and eventually broke off in solution. The Fe tip was sealed with epoxy and exposed using the same method as described for the Mn electrode in the main text. Vertical scanning interferometry images of the final Fe tip electrode are shown in Figure S3 with a tip diameter of ~110 μm.

As with the Mn system, approach curves (Figure S4) were performed by holding the tip electrode at a negative potential (-0.77 V vs. Ag/AgCl) where Fe oxidation does not occur, but hydrogen evolution does occur. The same 2 mm diameter Pt substrate electrode was used to collect the generated H₂ with an applied potential on the substrate of +0.1 V vs. Ag/AgCl, and the approach rate was 0.5 μm s⁻¹. Similarly with the Mn system, the solution used was a 4.5 mM HBF₄ aqueous solution with a 0.1 M NaBF₄ supporting electrolyte. As shown in Figure S4 the total collection efficiency obtained for the Fe experiment was 90%.

Since the Fe electrode was more disk-shaped than the Mn electrode it was possible to simulate the approach curve using a 2D axial symmetric simulation as opposed to a 3D

simulation. Figure S5 shows the simulated approach curve obtained using the same parameters as the Mn system described above, along with our experimental approach curve. Using the simulation we were able to measure a tip/substrate distance of 53 μm .

After the tip was positioned close to the substrate, LSV was performed on the tip sweeping the potential from -1.1 V to -0.4 V vs. Ag/AgCl at 5 mV s^{-1} while holding the potential of the Pt substrate at +0.1 V vs. Ag/AgCl. Figure S6 shows the tip and substrate current for this LSV experiment. The Fe tip current goes from the mass transfer controlled limiting current at high negative potentials, into the proton reduction wave at potentials around -0.7 V vs. Ag/AgCl, to Fe oxidation at potentials more positive than -0.5 V vs. Ag/AgCl. On the substrate, H_2 collection occurs at all potentials more negative than approximately -0.5 V vs. Ag/AgCl.

Figure S7A shows the total tip current, the inverted substrate current which represents the portion of the tip current that contributes to H_2 evolution, and the difference between the tip current and inverted substrate current which is the portion representing iron oxidation. From the approach curve we were able to obtain a 90% collection efficiency at the final distance of 53 μm . Figure S7B shows the corrected values of the hydrogen evolution current and iron oxidation current, accounting for the 90% collection efficiency.

To obtain the kinetic rate information, 2D axial symmetric COMSOL simulations were performed and fit to the experimental data for hydrogen evolution on Fe (Figure S8). Using the same procedure outlined above, we obtained a k_{eff}^0 value of $3.2 \times 10^{-5} \text{ cm}^2 \text{ s}^{-1}$ and an α of 0.35 for proton reduction on Fe. As was the case for Mn, to obtain an exchange current density for proton reduction on Fe in strong acid, we simulated Tafel curves in 1 M and 0.1 M acid (Figure S9). This was done by creating a 1D COMSOL Multiphysics simulation and simulating a potential sweep using Butler-Volmer kinetics for the flux boundary conditions. From the simulation

results, Tafel lines were drawn to obtain the exchange current densities. In 1 M acid we found a $\log(j^0)$ of -5.3 A cm^{-2} and in 0.1 M acid we found a $\log(j^0)$ of -6.8 A cm^{-2} . Averaging these two results gave us a $\log(j^0)$ of $-6.0 \pm 0.8 \text{ A cm}^{-2}$. This agrees very well with the known value of $\log(j^0)$ of -5.8 A cm^{-2} .

Supporting Figures

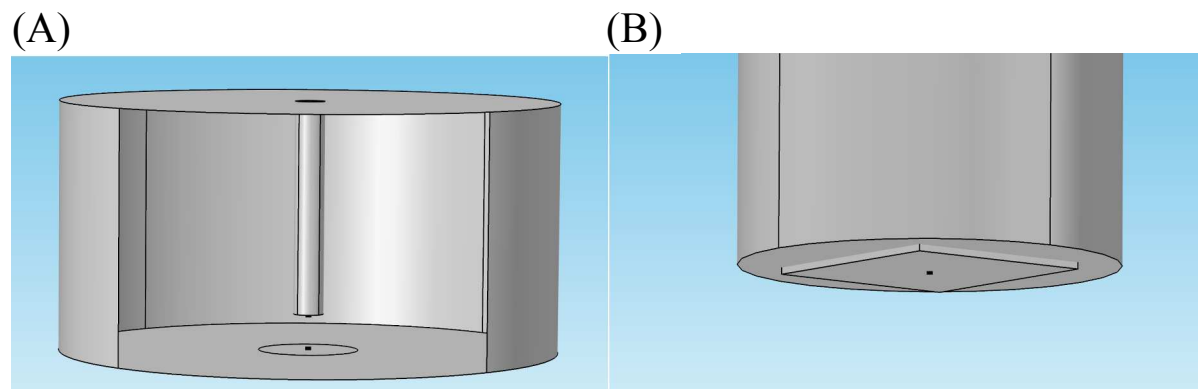


Figure S1. Entire 3-dimensional geometry (A) along with a portion highlighting the size and protrusion of the tip electrode (B). By using a 3-dimensional geometry we were able to simulate the exact size, shape, and protrusion of our rectangular electrode.

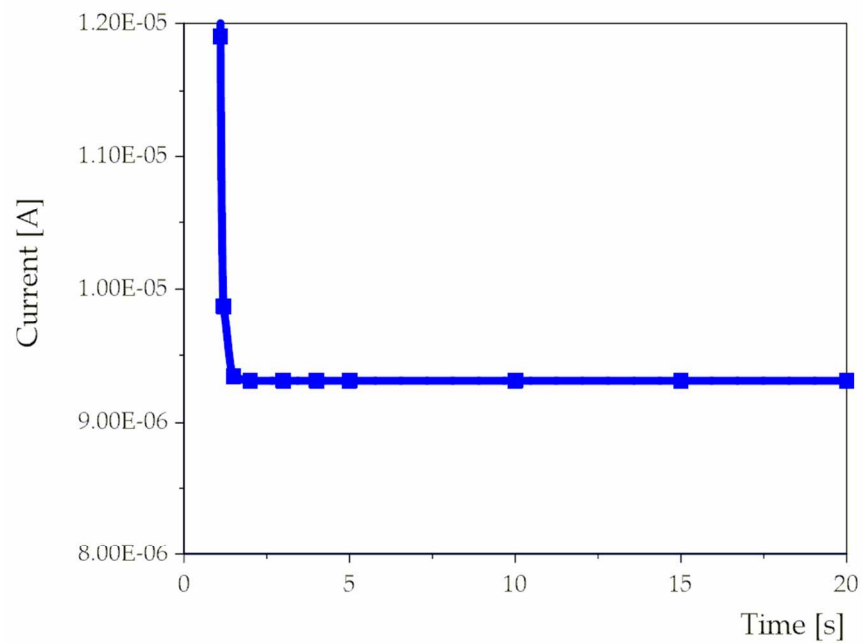


Figure S2. 3D COMSOL Multiphysics simulation showing tip current vs time for the square Mn electrode system under feedback at a tip/substrate distance of 65 μm . A steady-state tip current is reached after several seconds.

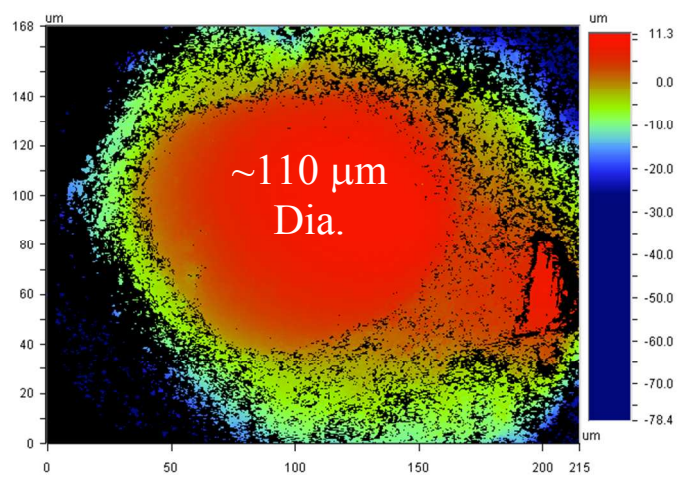


Figure S3. Vertical scanning interferometry image of Fe tip electrode. The diameter of the Fe tip is ~110 μm.

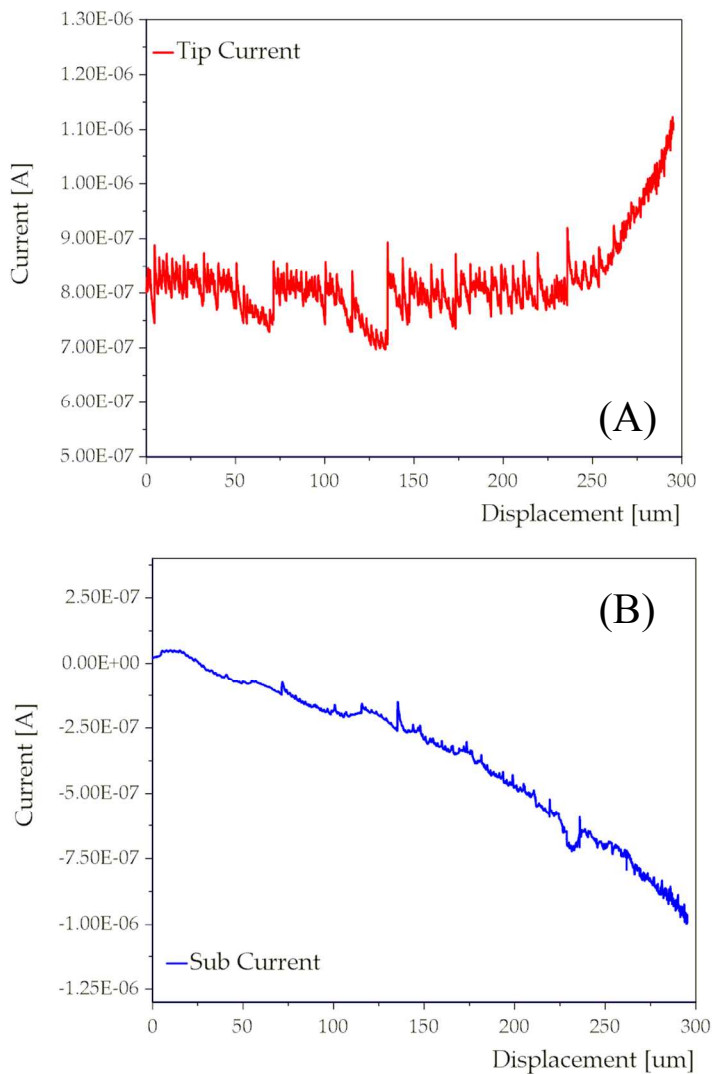


Figure S4. Tip current (A) and substrate current (B) for the approach curve with an Fe tip electrode and Pt substrate electrode in an aqueous solution of 4.5 mM HBF₄ with 0.1 M NaBF₄ supporting electrolyte. The tip potential was held at -0.77 V vs. Ag/AgCl to prevent Fe oxidation and the substrate potential was held at +0.1 V vs. Ag/AgCl. The total collection efficiency obtained at the minimum distance was 90%.

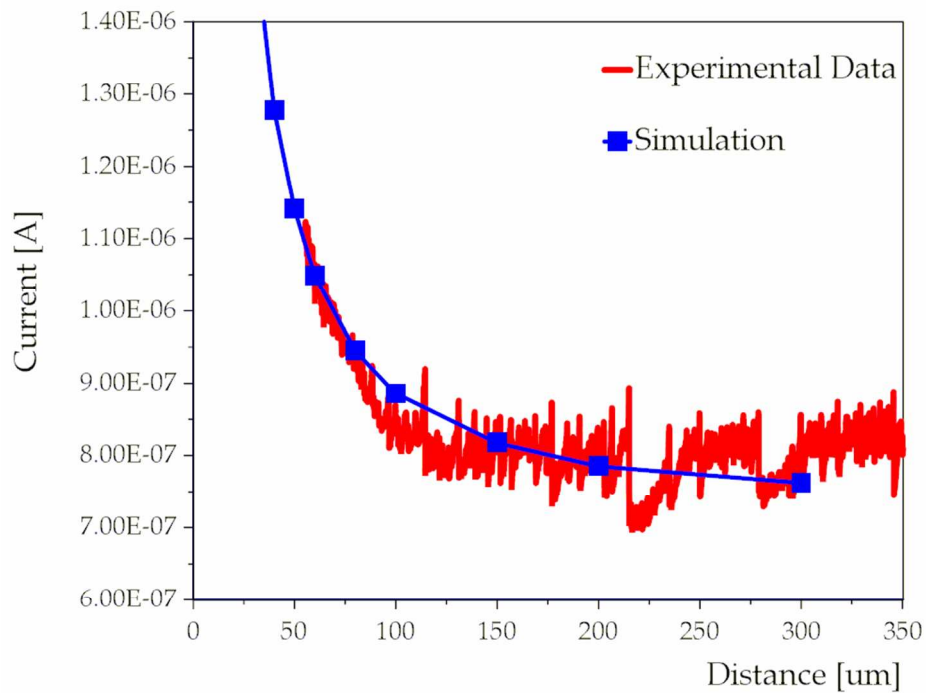


Figure S5. Experimental approach curve along with the COMSOL simulation of approach curve. Fitting the experimental approach curve to the simulation, the final tip/substrate distance was determined to be 53 μm .

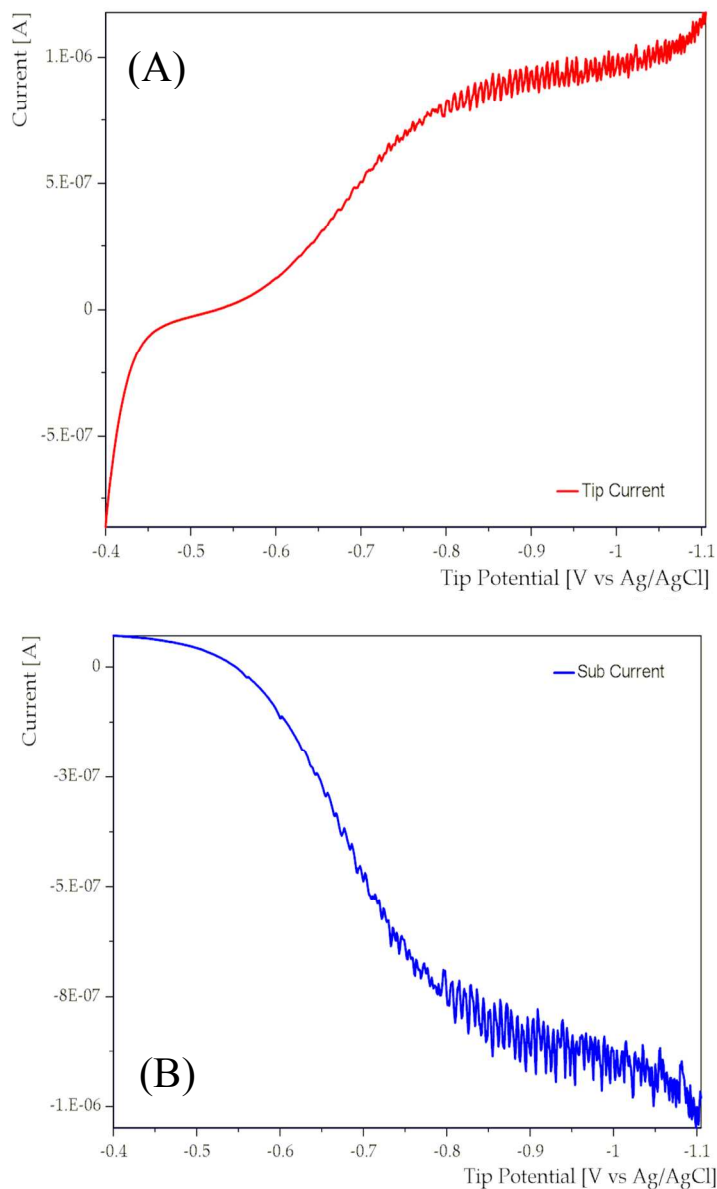


Figure S6. Linear sweep voltammetry showing the tip current (A) and substrate current (B) vs. tip potential. The tip was swept from -1.1 V to -0.4 V vs. Ag/AgCl at 5 mV s^{-1} while the tip was held at +0.1 V vs. Ag/AgCl. The tip current shows both hydrogen evolution and Fe oxidation while the substrate current shows hydrogen collection.

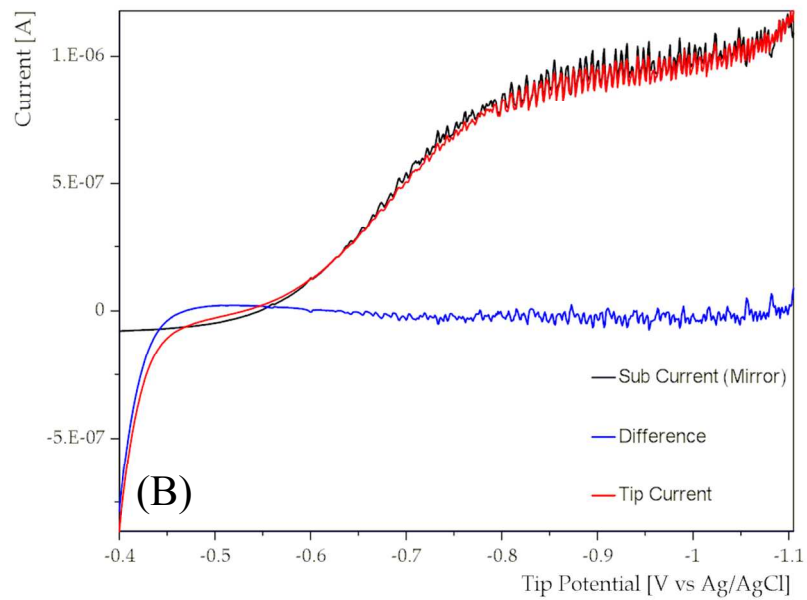
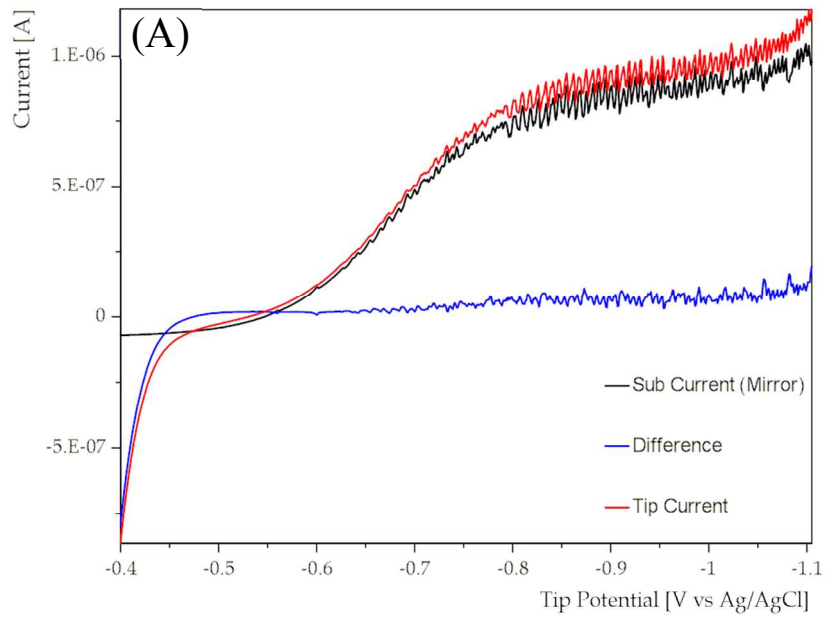


Figure S7. The total tip current along with the portions that are related to proton reduction and Fe oxidation as a function of tip potential for a linear sweep voltammetry experiment using a Fe tip electrode and Pt substrate electrode in 5 mM HBF₄ + 0.1 M NaBF₄. The substrate potential was held at +0.1 V vs. Ag/AgCl while the tip potential was scanned from -1.1 V vs. Ag/AgCl to -0.4 V vs. Ag/AgCl at a scan rate of 1 mV s⁻¹. The inverted substrate current is the portion of the current that results from the proton reduction reaction and the subtraction of the tip current from the inverted substrate current is the portion that results from the Fe oxidation reaction. (A) shows the raw experimental data while (B) corrects for the 90% collection efficiency.

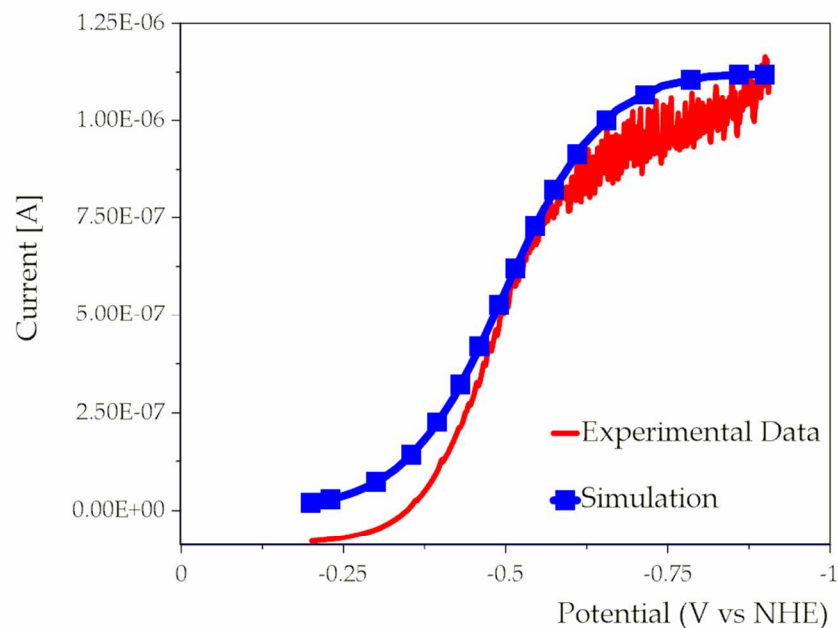


Figure S8. The experimental data for the portion of the current that is attributed to proton reduction on Fe, with a best fit simulation calculated using COMSOL Multiphysics. By fitting the simulation results to the experimental data we obtain kinetic rate constant parameters of $k_{\text{eff}}^0 = 3.2 \times 10^{-5} \text{ cm s}^{-1}$ and $\alpha = 0.35$.

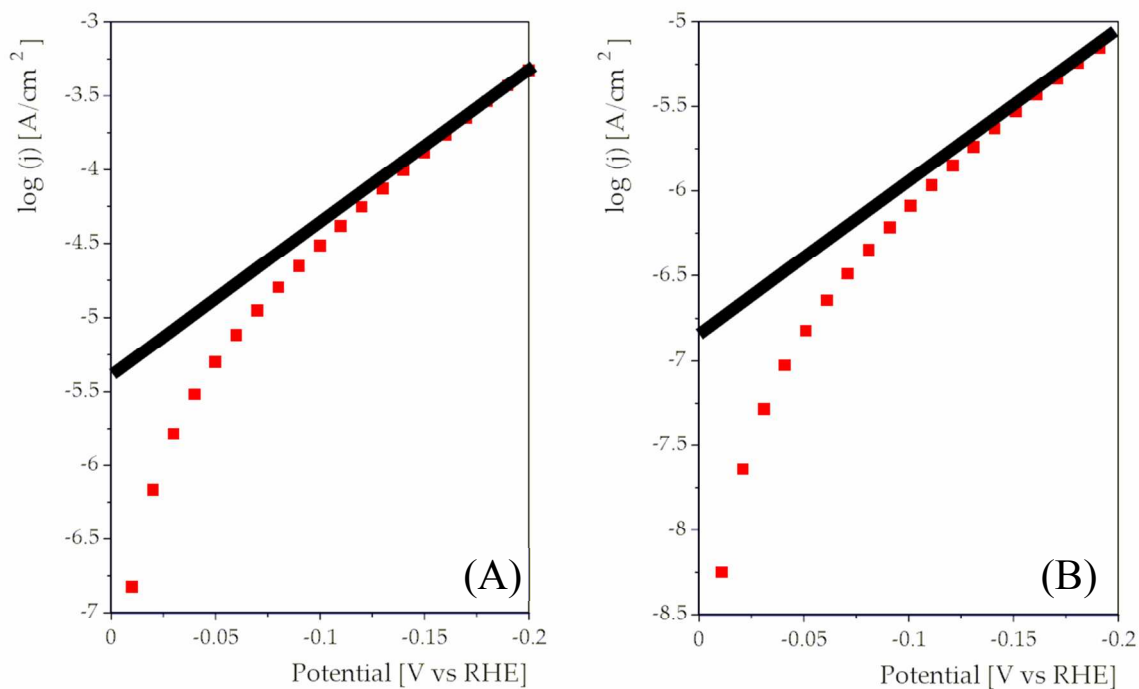


Figure S9. Simulations of Tafel curves using the kinetic rate constants obtained for Fe in acid concentrations of 1 M (A) and 0.1 M (B) to determine $\log(j^0)$ for proton reduction for Fe in strong acid. We determined that the average value of $\log(j^0)$ for proton reduction on Fe in strong acid to be -6.0 ± 0.8 A cm⁻².

Supplemental References

- ¹ Ferrell, R. T.; Himmelblau, D. M. *AIChE J.* **1967**, *13*, 702-708.
- ² Macpherson, J. V.; Unwin, P. R. *Anal. Chem.* **1997**, *69*, 2063-2069.
- ³ Martin, R. D.; Unwin, P. R. *J. Electronal. Chem.* **1997**, *439*, 123–136.
- ⁴ Kim, J.; Izadyar, A.; Nioradze, N.; Amemiya, S. *J. Am. Chem. Soc.* **2013**, *135*, 2321–2329.
- ⁵ Bard, A. J.; Mirkin, M. V., *Scanning Electrochemical Microscopy*. 2nd Ed.; CRC Press: Boca Raton, FL, **2012**, 26-30. Ed.; CRC Press: Boca Raton, FL, **2012**, 26-30.